Nanoscale

Accepted Manuscript

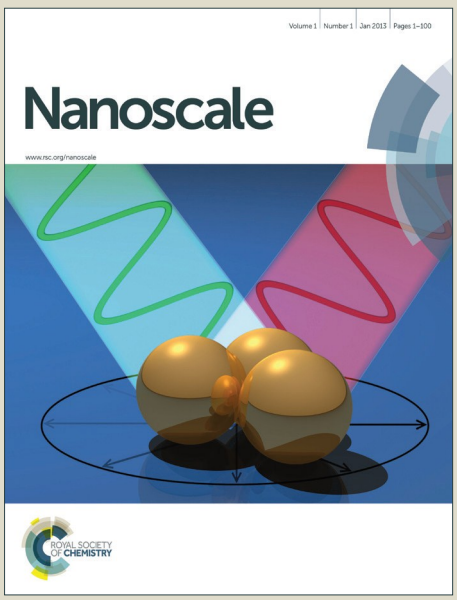

ROYAL SOCIETY OF CHEMISTRY

www.rsc.org/nanoscale

Nanoscale

RSCPublishing

COMMUNICATION

A switchable DNA origami nanochannel for regulating molecular transport at nanometer scale

Cite this: DOI: 10.1039/x0xx00000x

Dianming Wang, [a] Yiyang Zhang, [a] Miao Wang, [a] Yuanchen Dong, [a] Chao Zhou, [a] Mark Antonin Isbell,[a] Zhongqiang Yang, [a] Huajie Liu, [b] and Dongsheng Liu*[a]

Received 00th January 2012,
Accepted 00th January 2012

DOI: 10.1039/x0xx00000x

www.rsc.org/

A nanochannel with a shutter at one end was built by the DNA nanotechnology. Using DNA hybridization the shutter could be opened or closed, influencing the transport of materials through the channel. This process was visualized by an enzyme cascade reaction occurring in the structure.

Transmembrane protein channels play an important role in various biological processes, regulating the transport of materials and signals through biomembranes.[1] Therefore studying their operating mechanisms is vital for better understanding of life processes. Various artificial biomimetic nanochannels have been fabricated to mimic and simplify protein channels including: solid-state nanochannels made by drilling holes with focused ion beams, laser or chemically etched polymers or silicon membranes.[2] However, so far those technologies are not as accurate as biological nanochannels due to difficulties in controlling their dimensions.[3] In recent years, structural DNA nanotechnology, in particular DNA origami technology has proved to be a very efficient method to construct two to three dimensional, mono-dispersed, precisely addressable nanostructures,[4] and have furthered the development of artificial nanochannels.[5] In 2011, Keyser et al. constructed a conical DNA nanochannel that can be inserted into solid-state nanopores.[5a] The designed shape enabled the structure to fit into different pore sizes and make the inner effective pore size mono-dispersed. In the following year, Dietz and Simmel et al. published a syringe-shaped DNA origami nanochannel; by modifying cholesterol around the needle, the structure could penetrate and span a lipid membrane.[5b] Recently, several groups have used DNA tile structures, specifically DNA bundles, to fabricate nanochannels[5d, 5e] and studied their interactions with cancer cells.[5e] However, whilst these nanochannels based on structural DNA technology are mono-dispersed in diameter, they still lack another essential property of protein channels: controllable responsiveness.[6] Herein, we report an intelligent DNA nanochannel with a shutter at one end, which could be reversibly switched open and close, using the DNA chain exchange reaction. The opening and closing of the shutter influenced the transport of materials through this nanochannel and the processes have been visualized by an enzymatic cascade reaction[7] within the channel. This research not only provides a new strategy for preparing intelligent nanochannels, but also opens up new possibilities for studying material transport at the nanometer scale in restricted surroundings.

Our strategy is shown in Fig. 1. A DNA origami nanochannel was prepared by rolling up a rectangle origami[7c] with DNA sequences that can change their own conformations upon stimuli located on one side of the rectangle. With the formation of the nanochannel, the DNA strands turn into a responsive shutter at the end of cylinder. The detailed designs of the rectangle origami are shown in Fig. S1-S5. As the rectangle origami is not strictly a 2D plane, [4a, 7c] it preferred to roll up along its concave surface and keep a cylindrical shape with the help of sticky ends, placed as extensions, at the top and bottom helices. The nanochannel was 100 nm long and had a diameter of 22 nm following the size of the rectangle origami. Here, we added a row of 11 staple strands containing same 15-nt overhangs to one edge of the rectangle origami in an upright position to the concave side (Fig. S2). When rolled up, the 15-nt overhangs, called shutter strands, formed a shutter at the end of the nanochannel. As synthesized, according to earlier work, [2c, 2d] they are flexible and loosely packed at the edge of the DNA origami inner wall, and the nanochannel is considered open. By adding the single strand DNA (ssDNA) complementary to the 15-nt overhangs, called the lock strands, they hybridized with the overhangs forming rigid DNA duplexes. Due to the addition of possession length and the crowding effect, the efficient pore size of the nanochannel

Notes and references

a Key Laboratory of Organic Optoelectronics & Molecular Engineering of the Ministry of Education, Department of Chemistry, Tsinghua University, Beijing 100084, P. R. China. E-mail: liudongsheng@tsinghua.edu

b Laboratory of Physical Biology, Shanghai Institute of Applied Physics, Chinese Academy of Sciences, Shanghai 201800, China

† Electronic supplementary information (ESI) available: Experimental details including methods, materials, supporting figures and DNA sequences. See DOI: 10.1039/c000000x/

decreased, effectively closing the shutter. By synthesizing the lock strand with a mismatch at the 9th base from its 3' end and an 8-nt-toehold sequence at its 5' end, they could be displaced from the overhangs with their full complementary strands; named key strands, and as a result reopen the cylinder. We therefore constructed a DNA origami nanochannel equipped with a reversible shutter at one end.

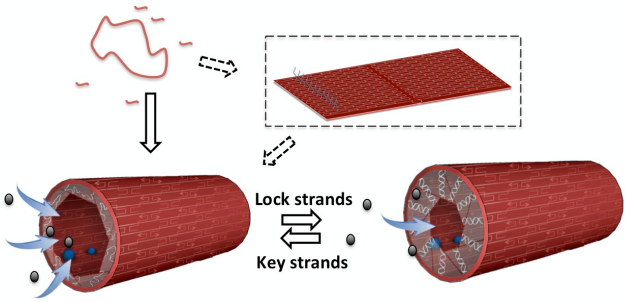

Fig. 1. Schematic illustration of reversible regulation of material entering the nanochannel by controlling the shutter open and closed. This DNA origami nanochannel is a scaffold for a model glucose oxidase-horseradish peroxidase (GOx-HRP) cascade reaction.

We first verified whether the nanochannel could be formed as designed. Fig. 2a and 2c show that structures containing shutter strands were obtained. Then we hybridized the nanochannel with lock strands modified with biotin at their 5' end. The bond between biotin and streptavidin was verified via atomic force microscopy (AFM). A group of six close placed dumb-bell loops that provide a height contrast under AFM imaging were positioned in the further corner from the enzymes of the nanochannel as a topographic index reference (Fig. S2 and S3) to unambiguously determine the relative positions of the shutter (Fig. 2). [8] A height increment of, ca. 2 nm, at the end of the cylinder and on the opposite side of the index, was visible in Fig. 2b. We concluded that the lock strands hybridized at the end of the nanochannel proving the shutter could be closed. It is worth mentioning that the streptavidin did not bind two biotins from different nanochannels together (Fig. S6). This suggests the shutter strands preferred pointing inwards to the channel instead of outwards in line with our design, the latter of which would have resulted in the bond of two cylinders side by side. Next we attempted to re-open the nanochannel by employing 23-nt-lock strands, containing mismatches at the 9th base and an 8-nt-toehold sequence, and hybridizing them with the shutter strands. The key strands hybridized with the lock strands, displacing them from the channel. As a result the shutter strands became single stranded, opening the shutter. This was verified by binding the streptavidin to biotinylated lock strands containing toeholds as previously described. The additional height at the end of the cylinder confirmed that the lock strands hybridized with the shutter strands (Fig. 2d). In contrast when the key strands displaced the biotinylated lock strands, the bond between streptavidin and biotin did not occur at the end of nanochannel, thus the height did not increase (Fig. 2e). These results show that we efficiently controlled the opening and closing of the DNA nanochannel as we designed.

We verified that the designed DNA nanochannel could modulate substance transport by immobilizing two cascade enzymes, glucose oxidase (GOx) and horseradish peroxidase (HRP), inside the channel. We theorized that the activity of the cascade reaction would be regulated by the opening and closing of the shutter. We therefore studied the efficiency of the enzymes in both cases. The enzymes used were immobilized within the structure following established methods.[7c] AFM here was used to character the enzyme-modulated nanochannels (Fig. S8). GOx was about 13 nm from the shutter, and HRP was an

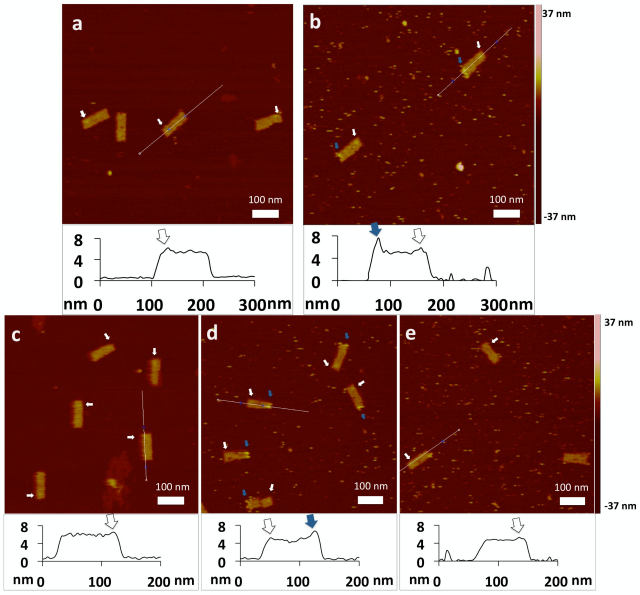

Fig. 2. AFM images and height profiles for DNA nanochannel. a) Open nanochannel; b) closed nanochannel, the height increment at the end of nanochannel in height profile was due to the bond between biotin (modified at the 5' end of lock strands) and streptavidin; c-e) the reversible open-closed-open state of nanochannel, respectively. The blue arrows highlight the height increment of the nanochannel at the closed end; the white arrows highlight the index on the nanochannel.

additional 15 nm from the former approximately. GOx catalyzes the oxidization of glucose generating gluconic acid and hydrogen peroxide. The latter is then catalytically reduced into water by HRP. The whole process can be visualized as 2'2'-azino-bis [3-ethylbenzthiazoline-6-sulphonic-acid] ($ABTS^{2-}$) turning into $ABTS^{\bullet-}$. The reaction was monitored in situ via UV-Vis spectroscopy. In order to close the nanochannel, a 10-fold excess of 15nt lock strands were added to hybridize with the shutter strands, forming rigid duplex DNA structures. Fig. 3a shows that the enzymes positioned within non-shuttered or open shuttered nanochannels exhibited much higher efficiencies than when freely dispersed in solution. It was likely due to both the distance and caging effect of the confined nanospace.[7c] There were no apparent differences in efficiencies between the non-shuttered and open shuttered nanochannels. It was attributed to the shutter strands being flexible single stranded DNA, allowing substances to flow freely into the nanochannel. In contrast when closed, the reaction efficiency decreased by about 28% after approximately 2000 s. This was due to the rigid DNA duplex partially blocking the entrance to the structure preventing the flow of substances into it. Furthermore, if the lock strands only contained 8 bases, meaning they only hybridized with 8nt at the bottom of the shutter strands leaving the shutter ajar, the efficiency of the reaction occurring in the nanochannel decreased by only about 8%. It further proved that the area blocked by the double

strands influenced the shuttering efficiency. These results indicated that the DNA shutters as designed could regulate the transport of molecular substances through the nanochannel.

We further tested the reversibility of the shutter mechanism through the sequential addition of 23-nt-lock and key strands, performing a cycle change: open-close-open, and monitored it via UV-Vis spectroscopy. We used a 2000 s increment to analyze the efficiency of the enzyme cascade reaction. We knew that when the lock strands were added the shutter closed by a dramatic decrease in absorbance as shown in Fig. 3b. This is in agreement with the data from Fig. 3a, which showed the closed nanochannel hindering the flow of substances and lowering the efficiency of the reaction. When key strands were added, the structure reopened and the efficiency of the reaction recovered. In addition, if the lock strands did not contain mismatches, the key strands only partially replaced the lock strands in our experiment condition, in which case the shutter was not fully opened and the efficiency of enzyme reaction was only partially recovered (Fig. S9 and S10). We concluded that adding lock and key strands could manipulate the nanochannel by opening and closing the shutter, and as such control substance transport in a reversible manner.

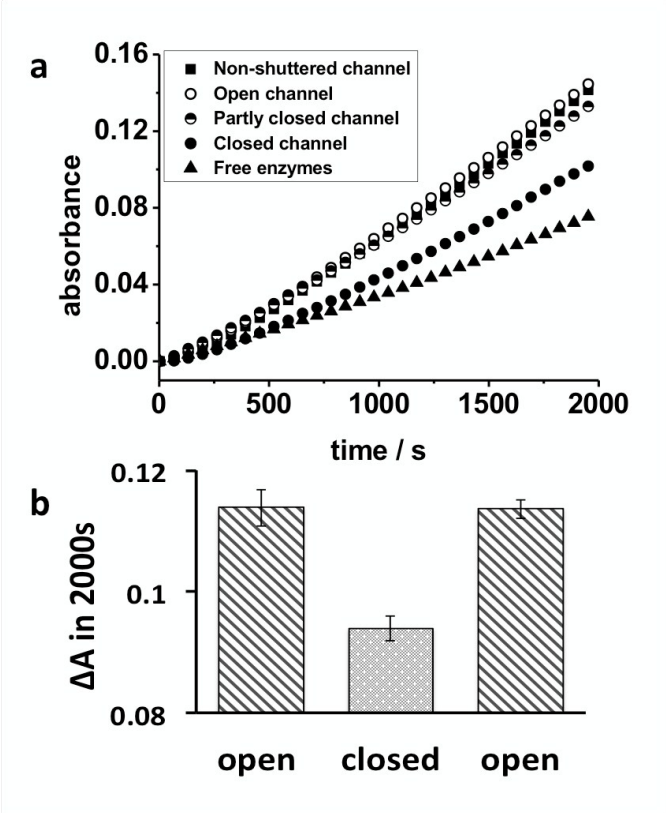

Fig. 3. a) Plots of product concentration vs time for different state nanochannels and free enzymes. GOx: HRP: DNA nanochannel = 1 nM: 1 nM: 0.5 nM. b) Absorbance increment of reaction in 2000 s controlled by the states of shutter in one cycle. The chart showed results obtained from three independent experiments.

Additionally, we placed the shutter on the opposite end of the channel further from the enzymes to study this influence on the cascade reaction efficiency. Both the number and sequence of the shutter strands were identical to the previous experiment. AFM characterization of the cylinder in Fig. 4a showed that the addition of biotinylated 15nt lock strands and streptavidin lead to a height increase at the end of nanochannel indicating the successfully placement of the shutter. Due to the distance between the shutter and the index was very close (Fig. S3), it was difficult to distinguish these two height increases in the height image of AFM. However, we could notice that there were two adjacent distinguishable peaks in the section analysis image. The higher one represented the closed shutter and the lower one was the index. It indicated the successfully placement of shutter on the same side of the index, or the opposite end of the enzymes. Just as before, real-time UV-Vis spectroscopy was used to monitor the enzyme cascade reaction efficiency (Fig. 4b). The forming of the rigid duplex DNA structures decreased the reaction efficiency as it hindered substrates from getting into the channel to be catalyzed by the enzymes. However, we found the reaction efficiency decreased by only about 16% after approximately 2000 s, much lower than in the previous experiment. Furthermore, we also placed the shutter on both ends of the nanochannel (Fig. S11a). It was consistent with speculation that the reaction efficiency showed the most significant decline, about 35%, in this condition by the real-time UV-Vis experiment (Fig. S11b). We concluded that it was facilitated for substrate molecular getting into the nanochannel to be catalyzed by enzymes through the entrance near from them. Most importantly, all these results showed the successful construction of a shuttered nanochannel based on DNA origami, which could regulate molecular transport at the nanometer scale.

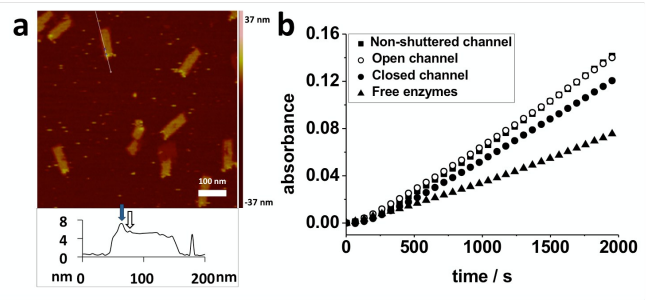

Fig. 4. The nanochannel with a shutter on the opposite end of the enzymes. a) AFM image and height profile for the closed DNA nanochannel. The blue arrows highlight the height increase of the nanochannel at the closed end; the white arrows highlight the index on the nanochannel. b) Plots of product concentration vs time for different state nanochannels and free enzymes. GOx: HRP: DNA nanochannel = 1 nM: 1 nM: 0.5 nM.

In order to show the scalability of the design, we also studied DNA nanochannel with a 12 nm diameter. Compared with the one with 22 nm diameters, the former had a greater hindrance due to its smaller pore size even though it only contained 5 shutter strands. AFM characterization of the 12 nm diameter cylinders in Fig. 5a showed that the addition of biotinylated 15nt lock strands and streptavidin lead to a height increase at the end of the nanochannel indicating it opened and closed. The real-time UV-Vis spectroscopy results in Fig. 5b; of the enzyme cascade reaction in the 12 nm diameter nanochannel showed a reaction efficiency decrease of about 46% when closed. These results suggest that by tuning the size of the pore, substance transportation can be further custom controlled.

It is worth noting that the shuttering efficiency was not 100% even with closed shutters at both ends of the nanochannel. Two

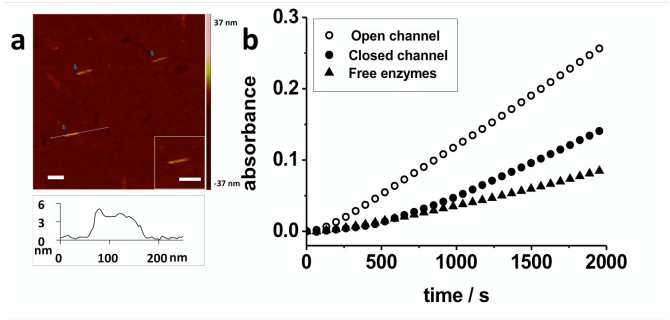

Fig. 5. 12 nm diameter nanochannel. a) AFM image and height profile for closed 12 nm diameter DNA nanochannel. b) Plots of product concentration vs time for different state nanochannels and free enzymes. GOx: HRP: DNA nanochannel = 0.5 nM: 0.5 nM: 0.5 nM. The scale bar is 100 nm.

possible non-mutually exclusive reasons are proposed: firstly, according to our design, the pore cannot be completely closed by the shutter (Fig. 1). To balance both the molecular crowding in the middle and loose packing near the edge, we chose eleven 15bp duplexes to form the closed shutter in a 22 nm nanochannel, leaving gaps between duplexes near the edges and a hole in the middle. This design enables reliable shutter operations by sacrificing some efficiency. However, the efficiency could be improved by different designs, for example: Xia and coworkers recently reported that cross-linked DNA superstructures could be more efficient gatekeepers for solid-state nanopores, [9] and we believe this strategy could also be easily applied to nanotubes fabricated by DNA origami technologies. Secondly, it is known that DNA origami is somewhat permeable to uncharged small molecules and even DNA single strands attached onto the origami.[10] This has been attributed to the low packing density of highly negatively charged DNA chains and the thermal fluctuations of DNA assemblies. Thus the substrates might leak into the DNA nanochannel via the hole on DNA origami wall. Nevertheless, this problem could be solved by wrapping the nanochannel with a lipid bilayer following a novel 'frame guided assembly' strategy, [11] or simply inserting the nanochannel into a solid-state nanopore similar to what Keyser has done.[5a]

Conclusions

In summary, we have successfully prepared an artificial, size mono-dispersed, responsive nanochannel with structural DNA nanotechnology, which retained two main characteristics of protein channels. This rational design can be summarized as a DNA nanochannel, formed by rolling up a 2D DNA origami sheet, with a built in molecular shutter, which works due to collective effects of several DNA hybridization. AFM was used to characterize and verify the successful construction of these structures. Upon DNA hybridization, the shutter could be opened and closed reversibly influencing the molecular transport through the channel. This process was visualized by a cascade enzymatic reaction, which was conveyed by two sequentially immobilized enzymes inside the channel. When the shutter was closed, the efficiency of cascade reaction in the nanochannel dropped, indicating the flow of substrate was obstructed. With established strategies, this smart DNA nanochannel also has the potential to be combined with solid-state nanopores[5a, 12] or inserted into lipid membrane[5b] to further mimic functions of natural protein channels, and be more responsive than its similar counterparts due to the design ability of DNA sequences. We believe that, this work provides not only an effective and simple strategy for constructing size mono-dispersed smart nanochannels, but also a platform for studying material transport at the nanometer scale in restricted surroundings.

Acknowledgements

We thank the National Basic Research Program of China (973 program, No. 2013CB932803) and the National Natural Science Foundation of China (Nos. 91427302, 21421064) for their financial support.

[1] a) E. Gouaux, R. MacKinnon, *Science* **2005**, *310*, 1461-1465; b) E. C. Yusko, J. M. Johnson, S. Majd, P. Prangkio, R. C. Rollings, J. Li, J. Yang, M. Mayer, *Nat Nano* **2011**, *6*, 253-260.
[2] a) J. Li, D. Stein, C. McMullan, D. Branton, M. J. Aziz, J. A. Golovchenko, *Nature* **2001**, *412*, 166-169; b) C. Dekker, *Nat Nano* **2007**, *2*, 209-215; c) F. Xia, W. Guo, Y. Mao, X. Hou, J. Xue, H. Xia, L. Wang, Y. Song, H. Ji, Q. Ouyang, *J. Am. Chem. Soc.* **2008**, *130*, 8345-8350; d) X. Hou, W. Guo, F. Xia, F.-Q. Nie, H. Dong, Y. Tian, L. Wen, L. Wang, L. Cao, Y. Yang, J. Xue, Y. Song, Y. Wang, D. Liu, L. Jiang, *J. Am. Chem. Soc.* **2009**, *131*, 7800-7805; e) X. Hou, W. Guo, L. Jiang, *Chem. Soc. Rev.* **2011**, *40*, 2385-2401.
[3] S. Hernández-Ainsa, U. F. Keyser, *Nanoscale* **2014**, *6*, 14121-14132.
[4] a) P. W. K. Rothemund, *Nature* **2006**, *440*, 297-302; b) P. Yin, R. F. Hariadi, S. Sahu, H. M. T. Choi, S. H. Park, T. H. LaBean, J. H. Reif, *Science* **2008**, *321*, 824-826; c) S. M. Douglas, H. Dietz, T. Liedl, B. Högberg, F. Graf, W. M. Shih, *Nature* **2009**, *459*, 414-418; d) A. V. Pinheiro, D. Han, W. M. Shih, H. Yan, *Nat. Nanotechnol.* **2011**, *6*, 763-772; e) T. Torring, N. V. Voigt, J. Nangreave, H. Yan, K. V. Gothelf, *Chem. Soc. Rev.* **2011**, *40*, 5636-5646; f) A. Kuzyk, R. Schreiber, H. Zhang, A. O. Govorov, T. Liedl, N. Liu, *Nat. Mater.* **2014**, *13*, 862-866; g) S. Kocabey, S. Kempter, J. List, Y. Xing, W. Bae, D. Schiffels, W. M. Shih, F. C. Simmel, T. Liedl, *ACS Nano* **2015**, *9*, 3530-3539; h) Z. Yang, H. Liu, D. Liu, *Npg Asia Mater.* **2015**, *7*, e161.
[5] a) N. A. W. Bell, C. R. Engst, M. Ablay, G. Divitini, C. Ducati, T. Liedl, U. F. Keyser, *Nano Lett.* **2011**, *12*, 512-517; b) M. Langecker, V. Arnaut, T. G. Martin, J. List, S. Renner, M. Mayer, H. Dietz, F. C. Simmel, *Science* **2012**, *338*, 932-936; c) M. Endo, R. Miyazaki, T. Emura, K. Hidaka, H. Sugiyama, *J. Am. Chem. Soc.* **2012**, *134*, 2852-2855; d) J. R. Burns, K. Göpfrich, J. W. Wood, V. V. Thacker, E. Stulz, U. F. Keyser, S. Howorka, *Angew. Chem. Int. Ed.* **2013**, *52*, 12069-12072; e) J. R. Burns, N. Al - Juffali, S. M. Janes, S. Howorka, *Angew. Chem. Int. Ed.* **2014**, *53*, 12466-12470; f) K. Göpfrich, T. Zettl, A. E. C. Meijering, S. Hernández-Ainsa, S. Kocabey, T. Liedl, U. F. Keyser, *Nano Lett.* **2015**, *15,* 3134-3138.
[6] a) F. Tombola, M. M. Pathak, E. Y. Isacoff, *Annu. Rev. Cell Dev. Biol.* **2006**, *22*, 23-52; b) I. Bahar, T. R. Lezon, A. Bakan, I. H. Shrivastava, *Chem. Rev.* **2009**, *110*, 1463-1497.
[7] a) J. Müller, C. M. Niemeyer, *Biochem. Biophys. Res. Commun.* **2008**, *377*, 62-67; b) O. I. Wilner, Y. Weizmann, R. Gill, O. Lioubashevski, R. Freeman, I. Willner, *Nat. Nanotechnol.* **2009**, *4*, 249-254; c) J. Fu, M. Liu, Y. Liu, N. W. Woodbury, H. Yan, *J. Am. Chem. Soc.* **2012**, *134*, 5516-5519; d) Y. Fu, D. Zeng, J. Chao, Y. Jin, Z. Zhang, H. Liu, D. Li, H. Ma, Q. Huang, K. V. Gothelf, *J. Am. Chem. Soc.* **2012**, *135*, 696-702; e) L. Xin, C. Zhou, Z. Yang, D. Liu, *Small* **2013**, *9*, 3088-3091.
[8] S. Rinker, Y. Ke, Y. Liu, R. Chhabra, H. Yan, *Nat. Nanotechnol.* **2008**, *3*, 418-422.
[9] W. Guo, F. Hong, N. Liu, J. Huang, B. Wang, R. Duan, X. Lou, F. Xia, *Adv. Mater.* **2015**, *27*, 2090-2095.
[10] N. Wu, D. M. Czajkowsky, J. Zhang, J. Qu, M. Ye, D. Zeng, X. Zhou, J. Hu, Z. Shao, B. Li, C. Fan, *J. Am. Chem. Soc.* **2013**, *135*, 12172-12175.
[11] a) Y. Dong, Y. Sun, L. Wang, D. Wang, T. Zhou, Z. Yang, Z. Chen, Q. Wang, Q. Fan, D. Liu, *Angew. Chem. Int. Ed.* **2014**, *53*, 2607-2610; b) Z. Zhao, C. Chen, Y. Dong, Z. Yang, Q.-H. Fan, D. Liu, *Angew. Chem. Int. Ed.* **2014**, *53*, 13468-13470; c) Y. Dong, Z. Yang, D. Liu, *Small* **2015**, *11,* 3768-3771.
[12] S. Hernández-Ainsa, N. A. W. Bell, V. V. Thacker, K. Göpfrich, K. Misiunas, M. E. Fuentes-Perez, F. Moreno-Herrero, U. F. Keyser, *ACS nano* **2013**, *7*, 6024-6030.

